Spectral line shape of resonant four-wave mixing induced by broad-bandwidth lasers

P. G. R. Smith* and P. Ewart
Clarendon Laboratory, University of Oxford, Parks Road, Oxford, OX1 3PU, United Kingdom
(Received 12 February 1996)

We present a theoretical and experimental study of the line shape of resonant four-wave mixing induced by broad-bandwidth laser radiation that revises the theory of Meacher, Smith, Ewart, and Cooper (MSEC) [Phys. Rev. A **46**, 2718 (1992)]. We adopt the same method as MSEC but correct for an invalid integral used to average over the distribution of atomic velocities. The revised theory predicts a Voigt line shape composed of a homogeneous, Lorentzian component, defined by the collisional rate Γ, and an inhomogeneous, Doppler component, which is a squared Gaussian. The width of the inhomogeneous component is reduced by a factor of $\sqrt{2}$ compared to the simple Doppler width predicted by MSEC. In the limit of dominant Doppler broadening, the width of the homogeneous component is predicted to be 4Γ, whereas in the limit of dominant homogeneous broadening, the predicted width is 2Γ. An experimental measurement is reported of the line shape of the four-wave-mixing signal using a broad-bandwidth, ''modeless,'' laser resonant with the $Q_1(6)$ line of the $A\ ^2\Sigma - X\ ^2\Pi(0,0)$ system of the hydroxyl radical. The measured widths of the Voigt components were found to be consistent with the predictions of the revised theory. [S1050-2947(96)02308-6]

PACS number(s): 42.65.−k

I. INTRODUCTION

Degenerate four-wave mixing, DFWM, is a nonlinear optical process that has found applications in areas ranging from high-resolution spectroscopy to adaptive optics. Spectroscopic applications are based on the enhancement of the signal when the incident laser fields are tuned to a resonance in the atomic or molecular medium. The sensitivity of DFWM, arising from the resonant enhancement, and the coherent nature of the generated signal, has been exploited to detect low concentrations of excited atoms [1] and molecular radicals in flames [2]. The application of DFWM to combustion diagnostics for measurements of minor species concentrations and temperatures has been recently reviewed [3]. The most widely used theory of DFWM in absorbing media, developed by Abrams and Lind [4], considers only the case of monochromatic lasers interacting with a system of two-level atoms. However, in many applications, pulsed, high power, tunable lasers are used to generate the DFWM signal. The output of these lasers inevitably has a finite spectral bandwidth with associated fluctuations of amplitude and phase in the electric field of the waves. Consideration of these fluctuations is important for a fully quantitative understanding of the DFWM signal. Furthermore, recent advances in multiplex DFWM use wide-bandwidth lasers to generate signals simultaneously on many molecular resonances for single-shot thermometry [5]. The effects of stochastic field fluctuations on interaction with matter is of considerable interest in its own right and is relevant to nonlinear optical processes other than DFWM. Bandwidth effects on resonance fluorescence [6], multiphoton absorption [7], and coherent anti-Stokes Raman scattering (CARS) [8,9] have been studied theoretically and experimentally. In the case of DFWM, the effects of laser bandwidth have also been studied with regard to the signal dependence on laser intensity and its saturation behavior [10] and also to the time dependence of signals in saturating fields [11]. More recently, a theory of the spectral line shape of broadband DFWM was presented by Meacher, Smith, Ewart, and Cooper [12], referred to hereafter as MSEC. In the present work we report a revision to the theory of MSEC to correct an invalid approximation made in the treatment of atomic motion effects. We also report on an experimental study of the line shape of broadband DFWM generated in the hydroxyl radical, OH. The results of this measurement are compared to the predictions of this revised theory relating to the homogeneous and inhomogeneous broadening processes.

II. THEORY

The basic theoretical approach to the problem has been presented previously, MSEC, [12] and so only the salient features will be outlined here for convenience. We consider the usual DFWM arrangement of counterpropagating pump beams having center frequency ω_1 and a bandwidth [full width at half maximum (FWHM)] of $2b$. The probe beam, crossing the pumps at a small angle, has a center frequency ω_3 and a bandwidth (FWHM) of $2p$. The fields are treated as plane waves defined as

$$\mathbf{E}_j(\mathbf{x},t) = \mathbf{A}_j \exp[-i(\omega_j t - \mathbf{k}_j \cdot \mathbf{x})] + \text{c.c.} \tag{1}$$

with $j = f,b,p,c$ for the forward pump, backward pump, probe, and signal, respectively. In this geometry the signal wave is the phase conjugate reflection of the probe wave. In a gas of two-level atoms these fields induce a polarization given by

$$\mathbf{P} = \sum_{m,n} \mathbf{P}^{m,n} \exp\{-i[m\omega_1 t + n(\omega_3 t - \mathbf{k}_3 \cdot \mathbf{x})]\}. \tag{2}$$

*Present address: Optoelectronics Research Centre, University of Southampton, Southampton, United Kingdom.

The polarization $\mathbf{P}^{2,-1}$ is related to the off-diagonal density matrix element $\rho_{eg}^{2,-1}$ by

$$\mathbf{P}^{2,-1}=N\boldsymbol{\mu}_{ge}\rho_{eg}^{2,-1}, \tag{3}$$

where N is the number density of the two-level atoms and $\boldsymbol{\mu}_{ge}$, is the electric-dipole matrix element connecting the ground g and excited states e.

The signal field amplitude is obtained from the nonlinear wave equation using the slowly varying envelope approximation to yield

$$\mathbf{A}_c(t)=\frac{2\omega_f-\omega_p}{\sqrt{2\epsilon_0 c}}\int_0^l dx\ \mathbf{P}^{2,-1}, \tag{4}$$

where l is the interaction length.

Hence the *intensity* of the signal wave is found to be

$$I_c(t)=\frac{(2\omega_f-\omega_p)^2|\boldsymbol{\mu}_{eg}|^2N^2}{2\epsilon_0 c}\times\int_0^l\int_0^l dx\ dx'\{\rho_{eg}^{2,-1}(x,t)[\rho_{eg}^{2,-1}(x',t)]^*\}. \tag{5}$$

When the fields in Eq. (1) are replaced by stochastic fields, such as those described by a phase-diffusion model (PDM) then this expression for the signal intensity must be correctly averaged over both spatial and temporal fluctuations. The product of density matrix elements, which is required, must be evaluated with due regard to the time orderings of the fields.

The heart of the problem is that the density matrix elements involve products of field terms with atomic terms and these products must be averaged over the field fluctuations. The solution to this problem lies in the use of a suitable decorrelation approximation. The crucial feature is that this decorrelation must be applied *simultaneously* to all the coupled equations involved in the determination of the final density matrix product. The simultaneous application of the decorrelation is necessary to preserve the effects of higher-order field correlations, which would be lost if the averaging were to be done before the products were evaluated. It is thus important to consider the problem in the time domain and so we use the equation of motion for the density matrix,

$$i\hbar\ \frac{\partial\rho}{\partial t}=[\hat{H},\rho]+\text{damping terms}, \tag{6}$$

where $\hat{H}$ is the Hamiltonian for the system. The energies of the two levels involved are denoted E_g and E_e for the ground and excited states, respectively. It is convenient to use a center frequency for the transition, where $\hbar\omega_{eg}=E_e-E_g$.

In the usual interaction picture the Hamiltonian is given by

$$\hat{H}=\hat{H}_0+\hat{V}.$$

$\hat{H}_0$ gives the unperturbed energy of the system and $\hat{V}$ is the interaction Hamiltonian where V is given by

$$V=\hbar\{\Omega(\mathbf{x},t)\exp(-i\omega_1 t)+\Omega_3(\mathbf{x},t)\exp(-i\omega_3 t)+\text{c.c.}\}$$

and where the Rabi frequencies Ω and Ω_3 are defined as

$$\Omega(\mathbf{x},t)=\frac{\mu_{eg}E}{2\hbar}$$

and

$$\Omega_3(\mathbf{x},t)=\frac{\mu_{eg}E_3}{2\hbar}.$$

The damping terms are introduced in the usual phenomenological way as κ and Γ, which represent the longitudinal and transverse relaxation rates, respectively. The transverse rate Γ is defined in terms of the longitudinal rate and the rate of dephasing collisions γ_0, as $\Gamma=\gamma_0+\kappa/2$.

In this treatment we use the phase-diffusing model, PDM, as discussed by Georges and Lambropoulos [13], where the electric field is defined as

$$E=E(t)\exp(i\omega t)+\text{c.c.}. \tag{7}$$

In the general case $E(t)=|E(t)|\exp[i\phi(t)]$. For the PDM the amplitude factor $|E(t)|$ is constant, and the phase of the wave, $\phi(t)$, is taken to be a Wiener process [14]. The decorrelation approximation is rigorous for the PDM and approximately true for the other field models in the limit of very large bandwidths and low intensity. Thus, in general, this model is not sensitive to the exact form of the higher-order statistics of the field. The four-wave mixing interaction is expected to depend on correlations of up to sixth order. While not exact for a real laser, the model provides a useful tool in the case of low intensity and large bandwidth.

To establish the link with earlier work, we note that the expansion of the equation of motion leads to a set of coupled differential equations for the density matrix elements as described in detail in Ref. [10] and also in MSEC. For convenience we reproduce these equations here:

$$\left[\frac{\partial}{\partial t}+\kappa\right]\rho_0(x,t)=\kappa-2\ \text{Im}[\Omega^*(x,t)\rho_1(x,t)], \tag{8}$$

$$\left[\frac{\partial}{\partial t}+\beta\right]\rho_1(x,t)=\frac{i}{2}\ [\Omega(x,t)\rho_0(x,t)+\Omega_3(x,t)\rho_4(x,t)], \tag{9}$$

$$\left[\frac{\partial}{\partial t}+c\right]\rho_3(x,t)=\frac{-i}{2}\ [\Omega_3^*(x,t)\rho_0(x,t)+\Omega^*(x,t)\rho_4(x,t)], \tag{10}$$

$$\left[\frac{\partial}{\partial t}+d\right]\rho_4(x,t)=i[\Omega^*(x,t)\rho_5(x,t)+\Omega(x,t)\rho_3(x,t)+\Omega_3^*(x,t)\rho_1(x,t)], \tag{11}$$

$$\left[\frac{\partial}{\partial t}+a\right]\rho_5(x,t)=\frac{i}{2}\ \Omega(x,t)\rho_4(x,t). \tag{12}$$

Note that we have used the abbreviated notation as follows:

$$\rho_0(x,t)\equiv\rho_{gg}^{0,0}(x,t)-\rho_{ee}^{0,0}(x,t),$$

$$\rho_1(x,t)\equiv\rho_{eg}^{1,0}(x,t),$$

$$\rho_2(x,t)\equiv[\rho_1(x,t)]^*,$$

$$\rho_3(x,t)\equiv\rho_{ge}^{0,-1}(x,t),$$

$$\rho_4(x,t)\equiv\rho_{gg}^{1,-1}(x,t)-\rho_{ee}^{1,-1}(x,t),$$

$$\rho_5(x,t)\equiv\rho_{eg}^{2,-1}(x,t);$$

and

$$a=\Gamma-i\Delta_4,$$

$$\beta=\Gamma-i\Delta,$$

$$c=\Gamma+i\Delta,$$

$$d=\kappa-i\delta,$$

$$\Delta_3=\Delta-\delta,$$

$$\Delta_4=\Delta+\delta,$$

$$\hbar\Delta=(\hbar\omega_1+E_g-E_e),$$

$$\delta=\omega_1-\omega_3.$$

Δ is the detuning of the pump waves from the atomic resonance and δ is the pump-probe detuning. We note also that a was defined incorrectly in MSEC.

The required quantity is the product,

$$\langle\rho_5(x,t)\rho_5^*(x',t)\rangle, \tag{13}$$

where the angle brackets represent averaging over both pump and probe fluctuations.

We define the density matrix products by

$$B_{ij}=\rho_i(x,t)\rho_j^*(x',t) \tag{14}$$

and so the required term is B_{55}. A differential equation for B_{55} can be defined with the aid of Eqs. (8)–(12) above, from which we derive the integral equation

$$B_{55}(x,x')=\int_{-\infty}^{t}\exp[-2\Gamma(t-t')]\frac{i}{2}[\Omega(x,t')B_{45}(x,x',t')-\Omega^*(x',t')B_{54}(x,x',t')]dt'.$$

Averaging over the field fluctuations is carried out using the decorrelation procedure as described in MSEC, yielding a set of equations that may be evaluated at the same time value, t. Using the time independence of the equations to evaluate the integrals leads to a set of simultaneous equations that are solved to give the DFWM reflectivity [10]. Having averaged over the temporal fluctuations of the field a spatial integration yields an expression for the reflectivity, R:

$$R=\frac{\kappa\vartheta^2}{4\Gamma^2}\frac{\Gamma+\kappa+p}{\Delta_2^2+(\Gamma+\kappa+p)^2}\times\frac{1}{\left[(1+2\vartheta)^{3/2}\left(1+\frac{\kappa\vartheta}{\Gamma}\right)^{1/2}\right]}\times\frac{1}{\left[(1+2\vartheta)\left(1+\frac{\kappa\vartheta}{\Gamma}\right)-2\frac{\kappa\vartheta^2}{\Gamma}\right]^{3/2}}, \tag{15}$$

where ϑ is the field-dependent term expressed in terms of the pump-induced Rabi frequency. This is Eq. (21) of Cooper *et al.* [10] and is valid at low intensity and for homogeneous broadening. For the case of inhomogeneous broadening, the solution is more complicated. An approximate solution was presented using an heuristic approach in Ref. [10]. The reflectivity R was found to scale as I_{pump}^2 for low intensity, but as I_{pump}^{-2} for intensities far above saturation levels. The signal was also found to be proportional to $b^{-2}p^{-1}$ at low intensity, corresponding to an intuitively reasonable dependence on the incident power per unit bandwidth.

This theory has been compared with Monte Carlo simulations by Agarwal *et al.* [15], who found good agreement for the saturation behavior of the reflectivity in the case of large bandwidths. For intermediate bandwidths the problem was found to be very sensitive to the higher-order statistics of the fields. Recent work by Williams *et al.* [16] has shown that the present model provides a significantly better quantitative description of the saturation characteristics of the DFWM reflectivity in the CH radical than the usual monochromatic theory. In this case the DFWM signal in flame CH was induced by a typical, pulsed, dye laser having a line width only slightly larger than that of the probed transitions.

III. SPECTRAL RESPONSE

The reflectivity or the intensity of the signal wave has been calculated by the procedure outlined above by evaluating the product of density matrix elements at one time value. The frequency spectrum, on the other hand, requires products of amplitudes at two different times, since the spectrum is related to the Fourier transform of the temporal autocorrelation of the signal wave amplitude. The signal frequency response, or spectral line shape, is thus determined by the product of density matrix elements at two times, say t and $(t+\tau)$.

A. Homogeneous broadening

The requirement for a product of density matrix elements evaluated at two times leads us to define a new expression for the B_{ij},

$$B_{ij}=\rho_i^*(x',t)\rho_j(x,t+\tau),$$

where the order has been swapped for the convenience of having the x' and the conjugate on the term independent of τ. The new B_{ij} is proportional to the autocorrelation of the signal amplitude. We exploit the fact that the problem we are considering is stationary and so, since $\langle B_{55}\rangle$ cannot be a function of t, but only of the relative delay τ, we write

$$\langle B_{ij}(x,x';\tau)\rangle=\langle\rho_i^*(x',0)\rho_j(x,\tau)\rangle.$$

As before, we derive an integral equation for the stochastically averaged product term:

$$\langle B_{55}(x,x';\tau)\rangle-\langle B_{55}(x,x';0)\rangle\exp(-a\tau)=\int_0^\tau\frac{i}{2}\langle\Omega(x,t)B_{54}(x,x',\tau)\rangle\exp[-a(\tau-t)]dt, \tag{16}$$

where we note that $\langle B_{55}(x,x';0)\rangle$ is simply the density matrix product term calculated in Sec. II. The set of equations determining the required product term is solved using a Laplace transform method as described in MSEC. We note here, for convenience, that the right-hand side of the Eq. (16) is a convolution. If we Laplace transform (represented by the symbol $\mathcal{L}$) both sides of the equation we obtain

$$(s+a)b_5(s)-\mathcal{B}_5(x,x')=\frac{i}{2}\,b_4(s), \tag{17}$$

where

$$b_5(s)=\mathcal{L}\langle B_{55}(x,x';\tau)\rangle,$$

$$b_4(s)=\mathcal{L}\langle \Omega(x,\tau)B_{54}(x,x';\tau)\rangle,$$

$$\mathcal{B}_5(x,x')=\langle B_{55}(x,x';0)\rangle.$$

As before, the averaging over the temporal fluctuations has to be conducted using a suitable decorrelation approximation. The products of density matrix terms at times differing by τ are reduced to simultaneous time products using the decorrelation procedure appropriate to the PDM. For example, averages of product terms at two different times are related to averages at a single time, say $t=0$ as follows:

$$\langle \Omega(\tau)B_{54}(0)\rangle=\langle \Omega(0)B_{54}(0)\rangle\exp(-b\tau)$$

and

$$\langle \Omega(\tau)\Omega^*(t)B_{55}(t)\rangle=2|\Omega|^2\langle B_{55}(t)\rangle\exp[-(b+d)(\tau-t)].$$

The power spectrum is found to be

$$P(\omega)=\mathrm{Re}\left[\frac{1}{s+a}\,\frac{1}{1+\dfrac{|\Omega|^2}{(s+a)(s+b+d)}}\right]_{s\to i(-\omega+\omega_{eg}+\Delta_4)}. \tag{18}$$

The rate a is equal to $\Gamma-i\Delta_4$ so the spectrum for low pump intensity $|\Omega|^2/b\kappa\ll 1$ is a simple Lorentzian with a full width at half maximum of 2Γ,

$$P(\omega)=\frac{\Gamma}{\Gamma^2+(\omega-\omega_{eg})^2}.$$

This is Eq. (19) of MSEC and is valid for the case of pure homogeneous broadening, but we would note here that it is not valid for large detunings as might be implied in MSEC.

B. Inhomogeneous broadening—the effect of atomic motion

We treat the effects of atomic motion that are responsible for Doppler broadening by defining a new, velocity-dependent, density matrix. This is expanded in terms of different velocity classes, and the averaging procedure is extended to include the summation over the velocity groups. Solutions to the velocity-dependent integral will be presented in the two limits corresponding first to the case where the homogeneous broadening dominates the Doppler effect, and second, where the Doppler broadening exceeds the homogeneous broadening—the Doppler limit.

Atomic motion results in an apparent shift in the frequencies of the incident fields such that $\omega_i\to(\omega_i\pm k_i\cdot v)$. Assuming the velocity distribution along the line of the axis defined by the intersecting beams to be Maxwellian, we define the new density matrix elements by integration over the velocity distribution $p(v)$,

$$\rho_{ij}=\int_{-\infty}^{\infty}p(v)\tilde{\rho}_{ij}(x,v,t)dv, \tag{19}$$

$$\tilde{\rho}_{ij}=\sum_{m,n}\rho_{ij}^{m,n}(x,v,t)\exp[-im_1(\omega_1 t-k_1x-k_1vt) -im_2(\omega_1 t+k_1x+k_1vt)-in(\omega_3 t-k_3x-k_3vt)]. \tag{20}$$

In this definition we explicity retain the indices labeling the forward and backward pump beams, m_1 and m_2, since a given atom will be affected by different Doppler shifts for interaction with each of these beams. The probability density for the longitudinal velocity distribution $p(v)$ is

$$p(v)=\frac{2\omega_{eg}}{c\Delta_d}\left[\frac{\ln 2}{\pi}\right]^{1/2}\exp\left[-\frac{4\omega_{eg}^2}{c^2}\,\frac{v^2\ln 2}{\Delta_d^2}\right], \tag{21}$$

where Δ_d is the Doppler width (FWHM). Similarly, we define a new, velocity-dependent, version of B_{ij},

$$B_{ij}(x,x';v,v';t,\tau)=\rho_i^*(x',v',t)\rho_j(x,v,t+\tau).$$

Following exactly the same Laplace transform procedure as before, keeping the v dependence, we obtain the following result for lowest order in Γ/b:

$$b_5(s;x,x';v,v')=\tilde{b}_5(s,v).\mathscr{B}_5(x,x';v,v'), \tag{22}$$

where

$$\tilde{b}_5(s,v)=\frac{1}{s+a+ik_3v}\,\frac{1}{1+\dfrac{|\Omega|^2}{(s+a+ik_3v)(s+b+d+ik_3v)}}. \tag{23}$$

The frequency spectrum is given by

$$P(\omega)=\lim_{s\to i(-\omega+\omega_{eg}+\Delta_4)}\mathrm{Re}\,\frac{\int_0^l\int_0^l\int_{-\infty}^{\infty}\int_{-\infty}^{\infty}p(v)p(v')b_5(s;x,x';v,v')dv\;dv'\;dx\;dx'}{\int_0^l\int_0^l\int_{-\infty}^{\infty}\int_{-\infty}^{\infty}p(v)p(v').\mathscr{B}_5(x,x';v,v')dv\;dv'\;dx\;dx'}. \tag{24}$$

In the previous work [12], it was assumed that the double integral over v and v' could be converted into one over $\Delta v = v - v'$. However, owing to the presence of the extra $b_5(s,v)$ in the numerator of this expression, this change of variables is not generally valid. In the general case it is necessary to change to new variables $\Delta v = v - v'$ and $v_{\rm av} = (v + v')/2$.

The effect of this new change of variables is seen by considering the product $p(v)p(v')dv\,dv'$. Rewriting $p(v)$ in a simplified form, removing the unnecessary constants gives

$$p(v) = \exp\left[\frac{-v^2}{\Delta_d^2}\right].$$

Using the first set of variables $\Delta v, v$, the product $p(v)p(v')$ is found to be

$$p(v)p(v') = \exp\left[-2\frac{v^2}{\Delta_d^2} + 2\frac{v\Delta v}{\Delta_d^2} - \frac{\Delta v^2}{\Delta_d^2}\right].$$

Thus, owing to the cross terms, we find that

$$p(v)p(v')dv\;dv' \neq p(v)p(\Delta v)dv\;d\Delta v,$$

whereas an equality was implied in MSEC. Using the new change of variables Δv and $v_{\rm av}$, we obtain

$$p(v)p(v')dv\;dv' = \exp\left[-2\frac{v_{\rm av}^2}{\Delta_d^2} - \frac{\Delta v^2}{2\Delta_d^2}\right]\frac{\partial(v,v')}{\partial(v_{\rm av},\Delta v)}dv_{\rm av}d\Delta v.$$

The Jacobian is equal to -1, so we see that $p(v)p(v')$ becomes the product of two Gaussians. The first has a Doppler width $\sqrt{2}$ smaller than normal and the second a Doppler width $\sqrt{2}$ larger than normal. This factor of $\sqrt{2}$ is new, and, as we shall see, leads to a Gaussian squared line shape. We can use the above result for the power spectrum, with appropriate approximations to derive an expression in terms of a Voigt profile for the physically important case of a broadband probe beam. We consider two limiting cases. The first case corresponding to a homogeneous width that is much larger than the Doppler width, $\Gamma \gg \Delta_d$, is trivial since, in this case, both the Gaussian terms act as Dirac δ functions, so that

$$p(v)p(v') = \delta(\Delta v)\,\delta(v_{\rm av}).$$

Both velocity integrals may be done by replacing all occurrences of v, v' by zero. The result is simply that of Sec. III A for homogeneous broadening.

C. The Doppler limit

We have considered the case of pure homogeneous broadening and we now turn to the second limiting case corresponding to the situation where the Doppler width is much larger than the homogeneous width. From a physical point of view, we would expect contributions to the signal arising from different velocity groups to add coherently only when the velocities differ by a small amount, typically a few homogeneous widths, Γ. The velocity-dependent product term $\mathscr{B}_{55}(x,x';v,v')$ has the form of a Gaussian numerator and a denominator with a number of simple poles and so we expect the result to be dominated by poles near $\Delta v = 0$. We proceed using the method of Cooper *et al.* [10] to treat the full set of coupled equations including the velocity-dependent terms. Restricting our contributions to poles near $\Delta v = 0$ allows us to eliminate many terms involving b in their denominators. Of the remaining terms, significant poles arise from the terms $\langle B_{55}\rangle$ and $\langle B_{00}\rangle$. We find

$$\langle B_{55}\rangle = \frac{i}{2\Gamma + ik_3\Delta v}\left[\langle\Omega(x)B_{45}\rangle - \langle\Omega^*(x')B_{54}\rangle\right], \qquad (25)$$

which contributes a pole to the final expression when $2\Gamma + 2ix = 0$, where $2x = k_3\Delta v$. Thus, this term leads to a pole at $x = i\Gamma$. After some tedious algebra we find also

$$\langle B_{00}\rangle = \frac{\langle\rho_0\rangle}{\left[(1+2\vartheta) - \kappa\vartheta^2\,\cos^2 k_1(x-x')\left(\dfrac{1}{\Gamma+\kappa\vartheta+ix} + \dfrac{1}{\Gamma+\kappa\vartheta-ix}\right)\right]}. \qquad (26)$$

This expression is simplified by considering that the effect of atomic motion will be to wash out the spatial modulation represented by the term $\cos^2 k_1(x-x')$ that can be replaced by its averaged value of 1/2. With this simplification we obtain

$$\langle B_{00}\rangle = \frac{\langle\rho_0\rangle[(\Gamma+\kappa\vartheta)^2 + x^2]}{(1+2\vartheta)\left[(\Gamma+\kappa\vartheta)^2 + x^2 - \dfrac{\kappa\vartheta^2(\Gamma+\kappa\vartheta)}{(1+2\vartheta)}\right]}, \qquad (27)$$

which provides poles at

$$x = \pm i(\Gamma+\kappa\vartheta)\sqrt{1 - \frac{\kappa\vartheta^2}{(\Gamma+\kappa\vartheta)(1+2\vartheta)}}.$$

If we assume a low intensity, we obtain poles at $x = \pm i(\Gamma + \kappa\vartheta)$ and note that in this case the pole in the upper half plane is at the same position as that from the B_{55} term.

The pole in the lower half plane at $x = -i\Gamma$ is the only one near the axis and so it is this pole that will be included in our contour for integration. In considering the integration over $v_{\rm av}$ we find that the contribution is dominated by the hierarchy

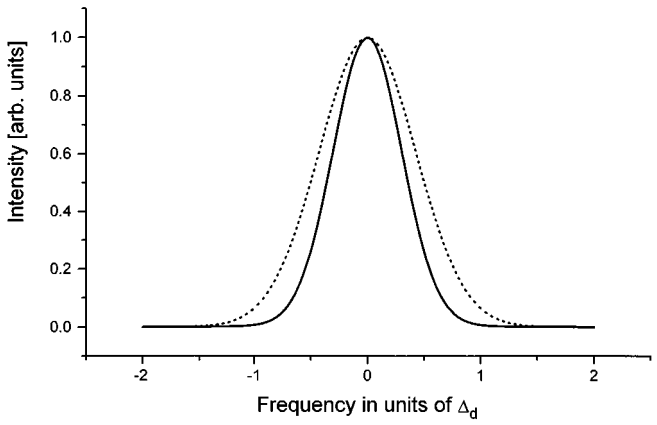

FIG. 1. Calculated line shape for broadband DFWM in the Doppler limit. A normal Voigt profile is shown, (dashed line), with a Doppler width $\Delta_d = 100\gamma$, where γ is the homogeneous width. The DFWM line shape (solid line) is seen to have a profile that is narrower by a factor of $\sqrt{2}$ than the corresponding normal Voigt line. The frequency scale is shown in units of Δ_d.

$$\langle B_{55}\rangle \rightarrow \langle \Omega B_{45}\rangle \rightarrow \langle B_{44}\rangle \rightarrow \langle \Omega_3^* \langle B_{14}\rangle\rangle \rightarrow \langle B_{11}\rangle \rightarrow \langle B_{00}\rangle \rightarrow \langle \rho_0\rangle .$$

Since the integral over v_{av} generates a width Δ_d, the contribution of other routes is reduced by a factor of at least $1/\Delta_d$. The $\langle B_{44}\rangle$ involves a term like $\mathrm{Re}\langle \Omega_3^* \langle B_{14}\rangle\rangle$. The evaluation of this term, including the averaging over the probe fluctuations, leads to a term like

$$\mathrm{Re}\langle \Omega_3^* \langle B_{14}\rangle\rangle = \mathrm{Re}\left(\frac{|\Omega_3|^2 \langle B_{11}\rangle}{p+\Gamma+\kappa+i\Delta_3+ix-ik_3 v_{\mathrm{av}}} \right).$$

We evaluate the integral for the power spectrum by assuming that the amplitude, or intensity, is essentially constant over the frequency range of the Doppler profile corresponding to small Δv. This is an approximation since we have to assume also that the Gaussian is sufficiently narrow to allow us to neglect contributions from denominators involving b. Finding the residue at the pole in the lower half plane by using the substitution $ix = \Gamma + \kappa\vartheta$, and using the new variables Δv and v_{av}, we find that to lowest order in $|\Omega|^2$, $b_5(s,v)$ becomes

$$b_5(s,\Delta v, v_{\mathrm{av}}) = \frac{1}{s+a+ik_3 v_{\mathrm{av}}+ix},$$

where we have also required $k_1 = k_3$, corresponding to the important condition of a small crossing angle. The v_{av} dependence of the integral over Δv is, for low intensity, found to be proportional to

$$\frac{\gamma_0}{(\Delta_3 - k_3 v_{\mathrm{av}})^2 + \gamma_0^2} \frac{1}{(s+a+ik_3 v_{\mathrm{av}}+\Gamma+\kappa\vartheta)}.$$

Making the usual substitution $s \rightarrow i(-w + w_{eg} + \Delta_4)$ we finally obtain an expression for the power spectrum:

$$P(\omega) = \mathrm{Re}\int_{-\infty}^{\infty} p(v_{\mathrm{av}})\, dv_{\mathrm{av}}\, \frac{\gamma_0}{(\Delta_3 - k_3 v_{\mathrm{av}})^2 + \gamma_0^2} \times \frac{1}{[2\Gamma + \kappa\vartheta + i(\Delta_3 - k_3 v_{\mathrm{av}})]}, \tag{28}$$

where

$$p(v_{\mathrm{av}}) = \frac{\sqrt{8}\,\omega_{\mathrm{eg}}}{c\Delta_d} \left[\frac{\ln 2}{\pi}\right]^{1/2} \exp\left[-\frac{8\omega_{eg}^2}{c^2} \frac{v_{\mathrm{av}}{}^2 \ln 2}{\Delta_d^2} \right].$$

This is similar to Eq. (24) of MSEC but has some important differences. Figure 1 shows the new result where we have plotted a normal Voigt profile, with a Doppler width of Δ_d (FWHM) and homogeneous width γ for comparison with the calculated DFWM line shape. The profiles are calculated for the case of dominant Doppler broadening where $\Delta_d = 100\gamma$ and the frequency scale is shown in units of one Doppler width. The main differences between this result and that of MSEC are that (i) The Doppler width is decreased by $\sqrt{2}$; (ii) for large probe bandwidth p, the line shape is a Voigt profile with a homogeneous contribution (FWHM) of 4Γ.

To summarize the results so far we note that we have considered two limiting cases. First, the case of pure homogeneous broadening is described by a simple Lorentzian of width 2Γ. Second, the case of dominant inhomogeneous broadening, arising from atomic motion, is described by a Voigt profile where the homogeneous component has a FWHM of 4Γ, i.e., twice that of the pure homogeneous case. As the homogeneous broadening increases, in relation to the Doppler width, we expect the width of the homogeneous component to tend to 2Γ. Our analysis here is not valid for such intermediate cases where the full integral over all velocity classes, including all possible combinations of m_1, m_2 would need to be evaluated. Such a calculation would probably require a numerical approach and has not been attempted here. In the second case where the Doppler width greatly exceeds the homogeneous width, the Gaussian component of the Voigt profile is found to be narrower by a factor of $\sqrt{2}$ than that of a simple Doppler broadened profile.

A simple physical understanding of these results may be gained by recalling that the four-wave mixing signal is the result of a *coherently* driven process. The radiating dipoles may add coherently only if their oscillation frequencies overlap within their *homogeneous* width. In the extreme Doppler limit, different velocity groups may radiate with very different center frequencies and so may not contribute coherently. A subgroup of atoms having velocity v_{av} has a homogeneous width of 2Γ and contributes coherently, in the integral over Δv, with a subgroup having a velocity $v_{\mathrm{av}} + \Delta v$, only if their homogeneous widths overlap. The Δv integral has the form of a convolution, and the convolution of two Lorentzians, of width 2Γ, is a Lorentzian of width 4Γ. When the Doppler width is much larger than the homogeneous width, the overall response is that of a product of two Gaussians. Since the two Gaussians have a negligible displacement in frequency from each other, the result is a Gaussian squared, which has a width smaller by a factor of $\sqrt{2}$ than a normal Doppler profile.

Finally, we note that a prediction was made in MSEC that a double-peaked line shape would result in the case of a

monochromatic probe detuned from the atomic line center. This prediction applied when the detuning was larger than the Doppler width. However, our calculation is not valid in this case and so the prediction for such large detunings of the probe must be considered invalid.

IV. BROADBAND DFWM LINE SHAPE MEASUREMENT

We report here a measurement of the spectral line shape of a DFWM signal induced by a broadband laser in the molecule OH. This is not the ideal choice of species with which to test a theory developed using a two-level atom model. However, the use of atomic vapors, having suitable absorption lines in the visible spectral region, poses problems of a different nature. In particular, it was found to be difficult to establish stable vapors of sufficiently low opacity to avoid serious absorption at line center. Molecular species have inherently weaker transition line strengths and are also of importance in applications of DFWM in combustion and plasma diagnostics. The radical OH is conveniently and reliably produced in a simple methane-air flame and has been detected in such an environment by DFWM [2]. Broadband DFWM of OH has also been used for flame thermometry [17,18] but the effects of the broadband excitation on the line shape have not been studied. In principle, measurements of the line shape may yield information on the temperature and pressure of the probed flame or plasma environment.

In this work we have generated DFWM signals using a broadband laser tuned to resonance with the $Q_1(6)$ line of the $A\ ^2\Sigma - X\ ^2\Pi(0,0)$ system in OH at 308.7338 nm. The important feature of this line, for our purpose, is that it is at least 10 cm^{-1} from any other strong line and so may be considered as an isolated transition. A weaker satellite line Q_{21} lies 1.5 cm^{-1} from the $Q_1(6)$ line at 308.7481 nm. The relative rotational transition probabilities are given by Dieke and Crosswhite to be in the ratio 50.4:4.0 [19]. The satellite is thus weaker but not negligibly so. The hyperfine structure is of the order of a few hundred MHz and so is negligible in relation to the spectral resolution obtained in this experiment.

The OH was produced in an approximately stoichiometric methane-air flame on a slot burner from an atomic absorption spectrophotometer. A maximum absorption of 30% was measured through the widest part of the flame above the primary reaction zone. Even with this level of absorption, no measurable effect was observed on the line shape. Line shape measurements were made in the base of the flame where the absorption was less than 5%. In separate measurements, the flame temperature was determined to be in the range 1700 to 2000 K [17].

Broadband laser light spanning the molecular resonance was generated by frequency doubling, the output of a ''modeless'' laser [20] pumped by a frequency-doubled Nd:YAG (neodymium-doped yttrium aluminum garnet) laser. This device provided an essentially continuous spectrum, without the longitudinal mode structure typical of conventional laser systems, and so better reproduced the type of laser spectrum modeled in the theory. The laser was spectrally tuned and narrowed using a 600-l/mm diffraction grating so that the frequency-doubled radiation had a linewidth of 13.3 cm^{-1}. The modeless laser used methanol solutions of sulfur rhodamine 640, and its output was amplified in two longitudinally pumped amplifier stages such that, after frequency doubling in a potassium dihydrogen phosphate (KDP) crystal, about 1.5 mJ of broadband laser light was available in the UV. In order to improve the beam quality, the UV beam was spatially filtered in a Keplerian telescope to give a fairly uniform beam profile of 4-mm diameter.

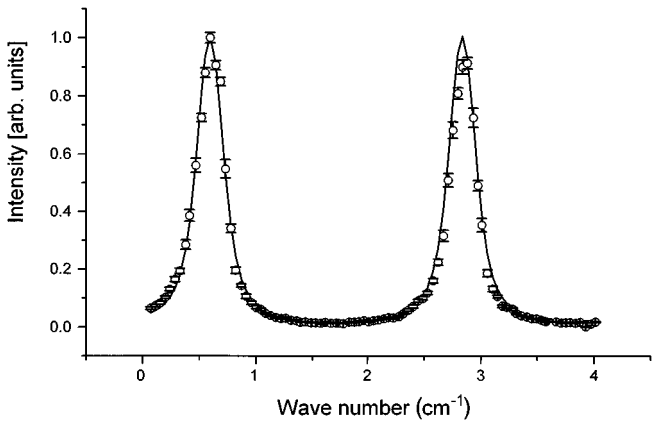

FIG. 2. Fabry-Perot interferogram of broadband DFWM signal spectrum generated in OH in an atmospheric pressure, methane-air flame. The open circles indicate the experimental data. The solid line shows a ''best-fit'' theoretical interferogram calculated using an assumed instrument function convolved with a DFWM line shape calculated using the present theory. The ''best-fit'' line shape corresponds to a temperature of 1750 K, in agreement with independent measurements of the flame temperature.

The usual phase conjugate geometry was used with counterpropagating pump beams and a probe crossing at an angle of approximately 3°. The backward pump beam was formed by retroreflecting the forward pump so that the optical delay between the two pumps exceeded the coherence length of the input laser pulses. This ensured that the two pump beams were uncorrelated. The DFWM signal was picked off by a 50% beam splitter placed in the probe beam and directed to a Fabry-Pérot interferometer (Burleigh Instruments RC150) approximately 5 m distant. The interferometer, having plates coated to give a reflectivity finesse of 40 at 308 nm, was used in the center-spot scanning mode to spectrally analyze the signal wave. The interference fringe pattern was imaged, using a 160-mm focal length silica lens, onto a 63-μm pinhole and the transmitted signal detected by a photomultiplier [(EMI) 9783B]. The photomultiplier signal was processed by a boxcar averager (Stanford Research SRS250) and the data stored on a personal computer. The energy of each laser shot was monitored by a pulse calorimeter and the result logged on a separate channel of the boxcar-computer system. The interferogram was recorded by measuring the center-spot intensity as a function of the plate separation, which was slowly varied by a ramp voltage applied to piezoelectric transducers that moved one plate of the interferometer while maintaining parallelism.

A. Results and discussion

The Fabry-Pérot interferometer was adjusted to give a free spectral range of 2.24 cm^{-1} to ensure that, with a maximum finesse of 40, the wings of the signal spectral line shape could be well resolved. This was important for discerning the

relative contributions of homogeneous (Lorentzian) and inhomogeneous (Gaussian squared) components of the Voigt profile. Unfortunately, no suitable source of sufficiently monochromatic radiation at 308 nm was available to allow a definitive measurement of the instrument function. Thus total confidence in the measurements is possible only when determining the upper limits of the linewidths. Errors arising from reduction of the finesse from the theoretical maximum (determined from reflectivity and flatness considerations) and other sources of broadening are discussed below.

An interferogram, showing two successive transmission peaks, is shown in Fig. 2. The error bars on the experimental points are determined largely by residual noise on the averaged data. The instrument function was modeled by a Lorentzian (based on a reflectivity finesse of 40) in order to calculate a theoretical interferogram. The calculated interferogram was derived from the theoretical line shape convolved with the assumed instrument function. A least-squares-fitting routine was used to obtain the ''best-fit'' theoretical line shape to the experimental data, and this is shown as the solid line in the figure. Assessing the quality of this fitting is difficult owing to the independent nature of the homogeneous and inhomogeneous components. A consideration of the variation of χ^2 with the two widths suggests a greater sensitivity to the homogeneous width.

The width of the inhomogeneous component was found to be 0.166 cm^{-1}. Assuming the factor of $\sqrt{2}$ in the Doppler width component, on the basis of the revised theory presented here, a flame temperature of 1750 K is inferred. This temperature is in reasonable agreement with that expected for the flame. A simple Gaussian component, i.e., neglecting the $\sqrt{2}$ factor, would yield a temperature of only 850 K. This result is highly improbable, since, at such a low temperature, there would be insufficient OH concentration to give a measurable signal. Thus the experimental data are consistent with the prediction of a ''Gaussian squared'' Doppler component in the line shape.

The question of the homogeneous contribution to the line shape is more problematic. The best-fit data of Fig. 2 yields a homogeneous width of 0.183 cm^{-1}. The collisional width is given by

$$\Gamma = \gamma_0 + \frac{\kappa}{2},$$

where γ_0 is the rate of dephasing collisions and κ is the upper-state population decay rate. The radiative lifetime of the upper state is of the order of 700 μs [21]. However, for OH in our flame environment, quenching collisions will dominate this decay rate [22]. Total collisional widths for OH, corresponding to 2Γ, have been measured for several colliders by Rea *et al.* [23,24] at a temperature of 2000 K. The dominant species are likely to be N_2, H_2O, and CO_2 for which the values of 2Γ were found to be 0.05 $cm^{-1}\,atm^{-1}$, 0.12 $cm^{-1}\,atm^{-1}$, and 0.04 $cm^{-1}\,atm^{-1}$, respectively. For a premixed propane-air flame at 1700 K, Dreier and Rakestraw [25] suggest a $2\Gamma = 0.07$ cm^{-1} and it is thus reasonable to assume this figure also for the flame used here. Thus the value of $4\Gamma = 0.14$ cm^{-1}, and this is in reasonable agreement, given the experimental uncertainties, with the value derived from the data of 0.18 cm^{-1}.

Errors and uncertainties arise in a number of aspects of the measurement. Absorption in the flame is potentially a serious effect. First, it could distort the spectrum of the incident laser light and thus invalidate the assumptions made regarding the fields in the theory. Second, absorption of the signal beam, would lead to a broadening and distortion of the line shape, as the absorption profile, being a simple Gaussian Doppler profile, would be different from that of the signal itself. However, as noted above, the measurements were made in a part of the flame where the absorption was measured to be less than 5% and so no significant broadening arising from absorption is expected. The largest uncertainty arises from ignorance of the instrument profile of the interferometer. The finesse factor of 40, set by the plate reflectivity, will be reduced by lack of parallelism of the plates. Vaughan [26] suggests that the effect of nonparallelism plates will be to add a Gaussian component to the instrument profile. This, in turn, will have the effect of increasing the measured Doppler width. Thus our measurements will indicate only an upper limit on the Doppler component. If the effect of nonparallelism was large, then a decrease in the free spectral range, by increasing the plate separation, would result in an apparent reduction in the measured linewidth. The fact that this was not observed indicates that the deviation from parallelism was not too significant. We estimate that other errors arising from the interferometer operation, including nonlinearity of the scanning and uncertainty in determination of the plate separation (free spectral range) amount to no more than 5%. This error is smaller than the uncertainty in the fitting of the data to the theoretical line shape.

Discrepancies between theory and experiment may arise since the medium used in these measurements cannot be considered as a pure ''two-level atom.'' The effects of rotational energy transfer by collisions or radiative (Raman) pumping have not been considered. However, the pulse energies used were low, relative to saturation levels, and so such Raman-type effects are not thought to be significant.

Finally, we note that the local environment of the OH probed could vary considerably over the measurement volume defined by the intersecting laser beams. Very steep gradients in both the OH concentration and temperature may be encountered in the flame. As a result, our measurement averages over the regions of different temperature and concentration. This effect is mitigated by the fact that the OH concentration is a very steep function of temperature T, and so only the hottest regions, between 1500 and 2000 K will contribute significantly. The variation of Doppler width over this range, since it scales with $\sqrt{T}$, will be small.

B. Conclusions

We have presented a revised theory of the line shape of resonant four-wave mixing induced by broadband laser fields. This work corrects for an invalid treatment of atomic motion in the previous work of MSEC. The main results of the corrected theory predict a Voigt-type line shape. In the limit where the broadening by atomic motion exceeds the homogeneous processes, the inhomogeneous component is given by a squared Gaussian, leading to a width, that is $\sqrt{2}$ smaller than the usual Doppler width. In this limit, the ho-

mogeneous component is found to have a width of 4Γ. In the case of dominant homogeneous broadening the width is predicted to be 2Γ.

Results of an experimental measurement of the line shape of DFWM in OH induced by a broadband ''modeless'' laser were found to be consistent with the predictions of the revised theory. A line shape was measured to have a Gaussian squared width of 0.17 cm^{-1} and a homogeneous component of width 0.18 cm^{-1}. Although only upper limits could be placed on these widths with quantitative confidence, the experimental uncertainties allowed values of the collisional widths and temperature to be derived, which were reasonable in view of published data on OH in similar flame environments.

The present experiments yielded data corresponding to only one combination of temperature and pressure in the atmospheric pressure flame. Work is currently underway in our laboratory to measure the broadband DFWM line shape in NO contained in a cell where temperature and pressure may be varied independently. These experiments should provide additional data to test the predictions of the theory regarding both Doppler broadening and the collisional contributions to the linewidth.

In principle, measurements of the broadband DFWM line shape could provide information, simultaneously, on the temperature and pressure in a flame or plasma environment that would be useful for combustion modeling and engineering-device optimization. DFWM in the forward-scattering geometry has also been shown to allow velocimetry of high-speed gas flows using the Doppler shift of the signal wave measured using a frequency-scanned narrowband laser [27]. Such signals generated by a broadband laser source would allow the Doppler shift to be determined in a single pulse. Such single-pulse methods are potentially useful in turbulent or transient flows. Experiments to test the feasibility of this technique are also currently underway in our laboratory.

ACKNOWLEDGMENTS

P.G.R.S. acknowledges with thanks the Engineering and Physical Science Research Council (UK) and British Gas PLC for financial support. P. Ewart is grateful to the Royal Academy of Engineering and British Gas PLC for financial support.

[1] P. Ewart and S. V. O'Leary, J. Phys. B **15**, 3669 (1982).
[2] P. Ewart and S. V. O'Leary, Opt. Lett. **11**, 279 (1986).
[3] R. L. Farrow and D. J. Rakestraw, Science **257**, 1894 (1993).
[4] R. L. Abrams and R. C. Lind, Opt. Lett. **2**, 94 (1978); *ibid.* **3**, 5(E) (1978).
[5] C. F. Kaminski, I. G. Hughes, G. M. Lloyd, and P. Ewart, Appl. Phys. B **62**, 39 (1996).
[6] H. J. Kimble and L. Mandel, Phys. Rev. A **15**, 689 (1977).
[7] D. E. Nitz, A. V. Smith, M. D. Levenson, and S. J. Smith, Phys. Rev. A **24**, 288 (1981).
[8] L. A. Rahn, R. L. Farrow, and R. P. Lucht, Opt. Lett. **9**, 223 (1984).
[9] S. Kroll, M. Alden, T. Berglind, and R. J. Hall, Appl. Opt. **26**, 1068 (1987).
[10] J. Cooper, A. Charlton, D. R. Meacher, P. Ewart, and G. Alber, Phys. Rev. A **40**, 5705 (1989).
[11] M. Kaczmarek, D. R. Meacher, and P. Ewart, J. Mod. Opt. **37**, 1561 (1990).
[12] D. R. Meacher, P. G. R. Smith, P. Ewart, and J. Cooper, Phys. Rev. A **46**, 2718 (1992).
[13] Georges A. T. and P. Lambropoulos, Phys. Rev. A **20**, 991 (1979).
[14] Athanasios Papoulis, *Probability, Random Variables and Stochastic Processes*, 3rd ed. (McGraw-Hill, New York, 1991).
[15] G. S. Agarwal, Gautam Vemuri, C. V. Kunasz, and J. Cooper, Phys. Rev. A **46**, 5879 (1992).
[16] S. Williams, R. N. Zare, and L. A. Rahn, J. Chem. Phys. **101**, 1093 (1994).
[17] I. P. Jefferies, A. J. Yates, and P. Ewart, in *Proceedings of the European Coherent Raman Spectroscopy Workshop, Florence 1992*, edited by E. Castelluci (World Scientific, Singapore, 1993).
[18] B. Yip, P. M. Danehy, and R. K. Hanson, Opt. Lett. **17**, 751 (1992).
[19] G. H. Dieke and H. M. Crosswhite, J. Quant. Spectrosc. Radiat. Transfer **2**, 97 (1962).
[20] P. Ewart, Opt. Commun. **55**, 124 (1985).
[21] K. R. German, J. Chem. Phys. **62**, 2584 (1975).
[22] R. P. Lucht, D. W. Sweeney, and N. M. Laurendeau, Appl. Opt. **25**, 4086 (1986).
[23] E. C. Rea, A. Y. Chang, and R. K. Hanson, J. Quant. Spectrosc. Radiat. Transfer **37**, 117 (1987).
[24] E. C. Rea, A. Y. Chang, and R. K. Hanson, J. Quant. Spectrosc. Radiat. Transfer **41**, 29 (1989).
[25] T. Dreier and D. J. Rakestraw, Opt. Lett. **15**, 72 (1990).
[26] J. M. Vaughan, *The Fabry-Perot Interferometer: History, Theory, Practice and Applications*, 1st ed. (Hilger, Bristol, 1989).
[27] R. B. Williams, P. Ewart, and A. Dreizler, Opt. Lett. **19**, 1486 (1994).